

Thermal conductivity of the Toda lattice with conservative noise

Alessandra Iacobucci¹, Frederic Legoll², Stefano Olla^{1,3} and Gabriel Stoltz³

¹: CEREMADE, UMR-CNRS 7534, Université de Paris Dauphine,

Place du Maréchal de Lattre de Tassigny, 75775 Paris Cedex 16, France

²: Université Paris Est, Institut Navier, LAM I, Projet MCMAC ENPC - INRIA,

6 & 8 Av. Pascal, 77455 Marne-la-Vallée Cedex 2, France

³: Université Paris Est, CERMICS, Projet MCMAC ENPC - INRIA,

6 & 8 Av. Pascal, 77455 Marne-la-Vallée Cedex 2, France

February 22, 2024

Abstract

We study the thermal conductivity of the one dimensional Toda lattice perturbed by a stochastic dynamics preserving energy and momentum. The strength of the stochastic noise is controlled by a parameter ϵ . We show that heat transport is anomalous, and that the thermal conductivity diverges with the length n of the chain according to $\kappa(n) \sim n^\alpha$, with $0 < \alpha \leq 2$. In particular, the ballistic heat conduction of the unperturbed Toda chain is destroyed. Besides, the exponent α of the divergence depends on ϵ .

1 Introduction

For a one dimensional system of length L , the thermal conductivity can be defined through the stationary flux of energy induced by connecting the system to two thermostats at different temperatures T_L and T_R . This flux of energy J_L is proportional to the difference of temperature $T = T_L - T_R$, and we define the thermal conductivity κ_L as

$$J_L = \kappa_L \frac{T}{L}. \quad (1)$$

If $\lim_{L \rightarrow \infty} \lim_{T \rightarrow 0} \kappa_L = \kappa$ exists and is finite, then the conductivity is normal and the system is said to satisfy Fourier's law [7]. The limit κ is the thermal conductivity of the system.

It is well known, by numerical experiments and certain analytical considerations, that the thermal conductivity diverges for one dimensional systems of oscillators with a momentum conserving dynamics [15, 14]. This is also consistent with some experimental results on the length dependence of the thermal conductance of carbon nanotubes [22, 10]. In the case of a chain of harmonic oscillators, J_L can be computed explicitly [19] and does not decrease when the size L of the system increases. This is due to the ballistic transport of energy carried by the non-interacting phonons, and it happens also for optical (pinned) harmonic chains, where momentum is not conserved. Ballistic transport of energy is expected for all systems whose dynamics is completely integrable [23], as for the Toda chain [20, 13].

Numerical evidence shows that non-integrability (whatever the definition of this concept one considers) is not a sufficient condition for normal conductivity, in particular for anharmonic chains of unpinned oscillators like the FPU model [14]. An energy superdiffusion is expected in these momentum conserving systems, and the thermal conductivity diverges as $\kappa_L \sim L^\alpha$, for some $\alpha \in (0; 1)$. There exists a wide debate in the physical literature about the existence or non-existence of one (or more) universal value of α [17, 15].

Stochastic perturbations of the dynamics have been introduced in order to understand these phenomena. A model where Langevin thermostats are attached to each oscillator in a harmonic chain was first introduced by Bolsterli et al [4]. This noise destroys all types of conservation laws, including energy, and the corresponding conductivity is finite (see [5] and [6] for the anharmonic case). Also, stochastic perturbations that preserve only the energy of the system give finite thermal conductivity [3].

The situation changes dramatically if the stochastic perturbation conserves both the energy and the momentum [1]. Such stochastic conservative perturbations model the chaotic effect of non-linearities. These systems may then be seen as completely non-integrable, since the only conserved quantities left are the energy and the momentum. In this case, at least for harmonic interactions, the thermal conductivity can be explicitly computed by the Green-Kubo formula. For unpinned models, it remains finite only in dimension $d \geq 3$, while it diverges when $d = 1$ or 2 . More precisely $\kappa \sim L^{\frac{1}{2}}$ when $d = 1$, and $\kappa \sim \log L$ when $d = 2$ [1, 2]. Analytical considerations for the same harmonic stochastic systems in non-equilibrium setting give the same results for the thermal conductivity computed according to (1), see [16]. For anharmonic interactions, rigorous upper bounds can be established, again by the Green-Kubo formula. In the one dimensional case, this leads to $\kappa \leq C L^{\frac{1}{2}}$.

These rigorous results motivated us to analyze the effect of stochastic perturbations on another completely integrable system, the Toda chain. The thermal conductivity of Toda lattices was already studied in [13], where it was shown that the ballistic energy transport is destroyed for a diatomic system. In contrast with the harmonic case where many computations can be performed analytically, the nonlinear dynamics considered here has to be solved numerically. We considered a chain in the nonequilibrium steady state setting, with two Langevin thermostats at different temperatures attached to its boundaries. We chose the simplest possible stochastic perturbation conserving both momentum and energy: each couple of nearest neighbor particles exchange their momentum at random times distributed according to an exponential law of parameter $\gamma > 0$.

Our main results are the following:

- A) As soon as some noise is present, i.e. $\gamma > 0$, the ballistic transport is immediately destroyed (as in the harmonic case) and energy superdiffuses, with $\kappa \sim L^{\frac{1}{2}}$ for $0 < \gamma \leq 2$;
- B) the exponent seems to depend on the noise strength γ , and is increasing with γ .

If A was somehow expected, B is quite surprising. It may be explained by the noise destroying some diffusive phenomena due to non-linearities, like localized breathers, with the result that current-current correlation decays slower when more noise is present. Besides, B suggests that any theory claiming the existence of a universal parameter γ has to be properly circumstanced.

This paper is organized as follows. The dynamics we consider is described in Section 2. The numerical simulations we performed are described in details in Section 3, whereas the obtained results are discussed in Section 4.

2 The stochastic dynamics

2.1 Description of the system

Hamiltonian. The configuration of the system is given by $\{q_i, p_i; i = 0, \dots, n\} \in \mathbb{R}^{2n+2}$, where q_i is the displacement with respect to the equilibrium position of the i -th particle, and p_i is its momentum. All masses are set equal to 1. The Hamiltonian is given by

$$H = \sum_{i=1}^n \frac{p_i^2}{2} + \sum_{i=1}^n V(q_i - q_{i-1}); \quad (2)$$

where the interaction potential is defined by

$$V(r) = \frac{a}{b} e^{-br} + ar + c; \quad (3)$$

and a, b, c are constants, $a > 0, b > 0$. Observe that if the product ab is kept constant, the harmonic chain is obtained in the limit $b \rightarrow 0$, while the hard sphere system is recovered as $b \rightarrow 1$. In our simulations, we chose $a = 1/b$ and $c = 1/b^2$ in order for V to be non-negative and to be minimal at $r = 0$. The potential is therefore determined by a single parameter b , which determines the strength of anharmonicity.

Boundary conditions. We set $q_0 = 0$, which amounts to removing the center-of-mass motion by attaching the particle at the left end of the system to a wall. However, we do not fix the total length q_n , and consider free boundary conditions on the right end. We checked that our numerical results are robust with respect to the boundary conditions. In particular, the same kind of scalings are obtained for fixed boundary conditions.

2.2 Description of the dynamics

The stochastic dynamics we consider has the following generator:

$$L = A + (B_1 + B_n) + S + \mathcal{E}_{p_n}; \quad (4)$$

where \mathcal{E} and \mathcal{E}_{p_n} are two positive constants. In (4), A is the Hamiltonian vector field:

$$A = \sum_{i=1}^N (p_i \mathcal{E}_{q_i} - \mathcal{E}_{q_i} H \mathcal{E}_{p_i}); \quad (5)$$

B_j are the generators of the Langevin thermostats attached at atom $j = 1$ and $j = n$:

$$B_j = T_j \mathcal{E}_{p_j}^2 - p_j \mathcal{E}_{p_j}; \quad (6)$$

and S is the generator of the random exchanges of momenta between nearest neighbor atoms: for any smooth function f ,

$$Sf(q; p) = \sum_{i=1}^{N-1} f(q; p^{i,i+1}) - f(q; p); \quad (7)$$

where $p^{i,i+1} \in \mathbb{R}^n$ is defined from $p \in \mathbb{R}^n$ by

$$p_i^{i,i+1} = p_{i+1}; \quad p_{i+1}^{i,i+1} = p_i; \quad (8)$$

and $p_j^{i,i+1} = p_j$ if $j \neq i, i+1$. Finally \mathcal{E} is the strength of a constant external force applied to the last particle n . In (6), we choose the temperatures $T_{j=1} = T_L$ and $T_{j=n} = T_R$.

2.3 Energy currents

We define the energy of the oscillator i for $1 \leq i \leq n-1$ as

$$E_i = \frac{p_i^2}{2} + \frac{1}{2} V(q_i - q_{i-1}) + V(q_{i+1} - q_i); \quad (9)$$

Locally the energy conservation is expressed by the stochastic differential equation

$$dE_i(t) = dJ_{i-1,i}(t) - dJ_{i,i+1}(t); \quad (10)$$

The energy currents $J_{i,i+1}(t)$ are the sum of contributions from the Hamiltonian and the stochastic mechanisms. For $i = 1, \dots, n-2$, the currents are

$$J_{i,i+1}(t) = \int_0^t \left(a_{i,i+1} + \sum_{s=i+1}^n ds + M_{i,i+1}(t) \right); \quad (11)$$

where $M_{i,i+1}(t)$ is a martingale,

$$a_{i,i+1} = \frac{1}{2} (p_i + p_{i+1}) V^0(q_{i+1} - q_i) \quad (12)$$

is the instantaneous Hamiltonian current, while

$$s_{i,i+1} = \frac{1}{2} p_i^2 - p_{i+1}^2 \quad (13)$$

is the instantaneous stochastic current (the intrinsic transport of energy due to the stochastic exchange). The martingale term $M_{i,i+1}(t)$ can be characterized in the following way: let $\{N_{i,i+1}(t)\}_{i=1}^{n-2}$ be independent Poisson processes of intensity λ . Then

$$M_{i,i+1}(t) = \int_0^t \frac{1}{2} p_i^2(s) - p_{i+1}^2(s) dN_{i,i+1}(s) \quad ds ;$$

where $p_i^2(s) = \lim_{t \downarrow s; t < s} p_i^2(t)$. At the boundaries of the system, the energy currents are

$$\begin{aligned} J_{0,1}(t) &= \int_0^t \frac{1}{2} T_1 p_1^2(s) ds + \int_0^t \frac{1}{T_1} p_1(s) dw_1(s) ; \\ J_{n-1,n}(t) &= \int_0^t \frac{1}{2} p_n^2(s) T_r + p_n(s) ds + \int_0^t \frac{1}{T_r} p_n(s) dw_n(s) ; \end{aligned}$$

where $w_1(t)$ and $w_n(t)$ are independent standard Wiener processes, and the last integrals on the right hand side of the previous formulas are Itô stochastic integrals.

2.4 The stationary state

If $T_1 = T_r = T$, we know explicitly the stationary probability measure of the dynamics, given by the Gibbs measure

$$\frac{e^{-(H + q_n)T}}{Z_n(T; \lambda)} \prod_{i=1}^n dr_i dp_i = \frac{e^{-B=T}}{Z_n(T; \lambda)} \prod_{i=1}^n e^{-(E_i + r_i)T} dr_i dp_i \quad (14)$$

where $r_i = q_i - q_{i-1}$ is the relative displacement, $Z_n(T; \lambda)$ is a normalization constant, and $B = p_n^2/2 + V(r_1) = 2 + V(r_n) = 2 - r_n$ is a boundary term.

If $T_1 \neq T_r$, there is no explicit expression of the stationary measure for anharmonic potentials. For certain classes of anharmonic potentials, the results of [18, 9] show that there exists a unique stationary probability measure. The assumptions on the potential made in [9] or similar works are not satisfied by the Toda potential (in particular, the growth at infinity is too slow in the limit $r \rightarrow +1$), but we believe that the techniques from [18, 9] can be extended to treat the case under consideration here.

We denote by $\langle \cdot \rangle$ the expectation with respect to this stationary measure, as well as the expectation on the path space of the dynamics in the stationary state. By stationarity we have

$$\langle J_{i,i+1}(t) \rangle = \langle a_{i,i+1} + s_{i,i+1} \rangle = \langle J_n \rangle$$

Because of energy conservation, J_n does not depend on i , but only of the size n of the system. Consequently,

$$J_n = \frac{1}{n-2} \sum_{i=1}^{n-2} a_{i,i+1} + \frac{1}{2} \frac{p_1^2 - p_{n-1}^2}{n-2} \quad (15)$$

In view of (1), the thermal conductivity can be defined by

$$\kappa_n(T; \lambda) = \lim_{\substack{T_1 \rightarrow T_r \\ T_r \rightarrow T}} \frac{n J_n}{T_1 - T_r} \quad (16)$$

It is clear from (15)–(16) that the direct contribution of the stochastic current to the conductivity is close to $\frac{1}{2}$ and remains bounded in n . Hence only the first term of (15), namely the Hamiltonian current

$$J_n^{\text{ham}} = \frac{1}{n} \sum_{i=1}^N \mathbf{x}_i^2 \mathbf{a}_{i,i+1}^a; \quad (17)$$

can be responsible for a possible divergence of the conductivity. In the sequel, we hence consider the conductivity

$$J_n^{\text{ham}}(T; \beta) = \lim_{\substack{T_1 \rightarrow T_r \\ T_r \rightarrow T}} \frac{n J_n^{\text{ham}}}{T_1 - T_r}$$

rather than (16). We are also motivated by the following numerical considerations. As reported in the sequel, we numerically observe that $J_n^{\text{ham}} \sim n^\alpha$ for some $\alpha \in (0; 1)$, hence $J_n^{\text{ham}} \sim n^\alpha$ for $\alpha \in (1/2; 1)$. As a consequence, the second term of (15) is indeed negligible with respect to the first term, in the limit $n \rightarrow \infty$. The regime of large n may yet be difficult to reach numerically, so that the stochastic current contribution in (15) may be small but not negligible compared with (17) for the considered values of n .

By a linear response theory argument, the thermal conductivity of the finite system can also be defined by a Green-Kubo formula:

$$J_n^{\text{GK}}(T; \beta) = \frac{1}{T^2} \sum_{i=1}^N \mathbf{x}_i^2 \mathbf{a}_{i,i+1}^a(t) \mathbf{a}_{i,i+1}^a(0) \int_0^\infty dt e^{-\beta t}; \quad (18)$$

where here the expectation $\langle \cdot \rangle_t$ is with respect to the dynamics starting with the equilibrium Gibbs measure given by (14) (we assume here that the integral (18) indeed exists).

In principle, for finite n , $J_n^{\text{GK}} \notin \mathbb{R}$, but we expect that they have, qualitatively, the same asymptotic behavior as $n \rightarrow \infty$.

3 Numerical simulations

3.1 Implementation

All the simulations performed in this work were done with $T_1 = 1.05$ and $T_r = 0.95$. This temperature difference is small enough so that the thermal conductivity around $T = 1$ should be approximated correctly. We also set the external force to $\mathbf{f} = 0$.

3.1.1 Integration of the dynamics

We denote by q_i^m, p_i^m approximations of $q_i(t_m), p_i(t_m)$ at time $t_m = m \Delta t$. The time-discretization of the dynamics with generator (4) is done with a standard splitting strategy, decomposing the generator as the sum of $A + (B_1 + B_n)$ and S .

The Hamiltonian part of the dynamics and the action of the thermostats on both ends of the

chain are taken care of by the so-called BBK discretization [8] of the Langevin dynamics:

$$\begin{aligned}
 p_i^{m+1/2} &= p_i^m - \frac{t}{2} r_{q_i} H(q_i^m) \\
 &\quad + \gamma_{i,1} \frac{t}{2} p_1^m + \frac{t}{2} T_1 G_1^m \\
 &\quad + \gamma_{i,n} \frac{t}{2} p_n^m + \frac{t}{2} T_r G_n^m ; \\
 q_i^{m+1} &= q_i^m + t p_i^{m+1/2} ; \\
 p_i^{m+1} &= p_i^{m+1/2} - \frac{t}{2} r_{q_i} H(q_i^{m+1}) \\
 &\quad + \gamma_{i,1} \frac{t}{2} p_1^{m+1} + \frac{t}{2} T_1 G_1^m \\
 &\quad + \gamma_{i,n} \frac{t}{2} p_n^{m+1} + \frac{t}{2} T_r G_n^m ;
 \end{aligned} \tag{19}$$

where $\gamma_{i,1}$ and $\gamma_{i,n}$ are Kronecker symbols and G_1^m, G_n^m are independent and identically distributed random Gaussian variables of mean 0 and variance 1. Notice that the last step in the algorithm, written as an implicit update of the momenta, can in fact be rewritten in an explicit manner. Alternatively, one can first integrate the Hamiltonian part of the dynamics with the Verlet scheme [21] using a time step t , and next analytically integrate the Ornstein-Uhlenbeck processes on the momenta at both ends of the chain, associated with the generator $(B_1 + B_n)$. In this work, we rather considered algorithm (19). We tested two different friction parameters, $\gamma = 1$ and $\gamma = 0.1$, to study how the results depend on the boundary conditions.

The noise term with generator S is simulated by exchanging p_i and p_{i+1} at exponentially distributed random times, with an average time τ_i^{-1} between two such exchanges. More precisely, we attach to each spring a random time τ_i^m , with τ_i^0 drawn from an exponential law with parameter τ_i^{-1} . This time is updated as follows: if $\tau_i^m < t$, then $\tau_i^{m+1} = \tau_i^m - t$, otherwise p_i and p_{i+1} are exchanged and τ_i^{m+1} is resampled from an exponential law of parameter τ_i^{-1} .

3.1.2 Initial conditions and thermalization

The initial conditions are chosen by imposing a linear temperature profile. We used to this end the Langevin dynamics of generator $L_{IC} = A + \mathcal{B}$, where A is given by (5), and

$$\mathcal{B} = \sum_{i=1}^N T_i q_{p_i}^2 - p_i q_{p_i} ; \quad T_i = \frac{n}{n-1} T_1 + \frac{i-1}{n-1} T_r ;$$

Once a linear temperature profile, obtained from the time-average of the local kinetic energy, is indeed obtained, the term \mathcal{B} is switched off, and replaced by $(B_1 + B_n) + S$. The dynamics with generator (4) is then integrated using the numerical scheme described in Section 3.1.1, and the spatially averaged instantaneous Hamiltonian current is monitored. At time $t_m = m t$, this current is defined as

$$j_m = \frac{1}{n} \sum_{i=1}^N \dot{q}_{i,i+1}^{a,m} ; \tag{20}$$

where the instantaneous Hamiltonian current $\dot{q}_{i,i+1}^{a,m}$ is defined as in (12), upon replacing $q_i(t)$ and $p_i(t)$ by their approximations q_i^m and p_i^m . The thermalization time is somehow loosely defined as the time after which the variations of the instantaneous current stabilize (see Figure 1 for an illustration). This time could be determined more carefully by estimating some local-in-time variance of the current, and requiring that this variance stabilizes.

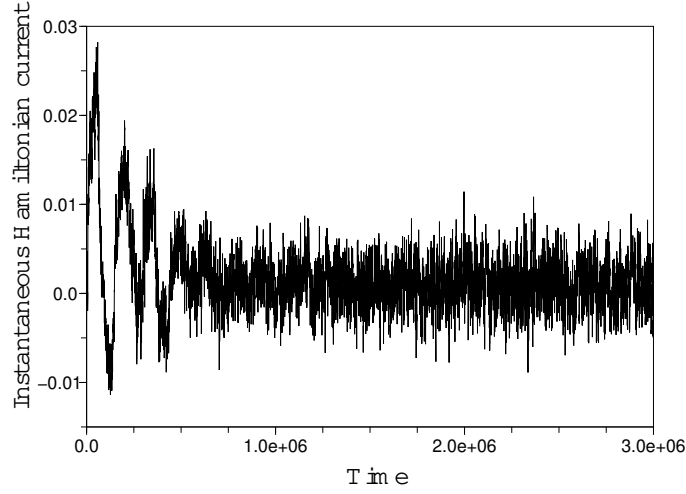


Figure 1: Instantaneous Hamiltonian current (20) as a function of time, in the case $b = 1$, $\gamma = 10^{-3}$, $\eta = 0.1$, $\tau = 0.05$, $n = 2^{16} = 65,536$. The thermalization time is $T_{\text{thm}} \approx 2 \times 10^6$.

3.1.3 Computation of the energy currents

Once some steady state has been reached, the instantaneous Hamiltonian current (20) is computed at each time step, and an approximation of the Hamiltonian current (17) is obtained as a time average:

$$\mathcal{J}_n^M = \frac{1}{M} \sum_{m=1}^M \mathcal{J}_n^m : \quad (21)$$

In the limit of a large number of iterations M and for a small time-step τ , we have $\mathcal{J}_n^M \approx \mathcal{J}_n^{\text{ham}}$. Using the current (21), we define the conductivity b_n^M and the exponent β by

$$b_n^M = \frac{n \mathcal{J}_n^M}{T_L - T_R} \quad n : \quad (22)$$

A priori, the exponent β depends on all the parameters of the model: the anharmonicity parameter b , the magnitude γ of the coupling to the end thermostats, the noise strength η , and the temperatures T_L and T_R . In our simulations, we have explored how the numerical results (and in particular the exponent β) depend on the first three parameters, and we have kept T_L and T_R fixed. We wish to point out that the results reported here already required an extremely large CPU time. Indeed, for the largest system considered ($n = 2^{17}$), several months were needed to integrate the dynamics with a small enough time step to ensure accuracy ($\tau = 0.05$ here), on a time $T = 10^7$ long enough such that convergence of the time average (21) is reached (see Section 3.2.2 for more details).

3.2 Error estimates

There are two types of error in the numerical estimation of the currents: a systematic error (bias) due to the time step error ($\tau > 0$), and a statistical error due to the finiteness of the sampling ($M < +\infty$). We consider successively these two issues.

3.2.1 Choice of time step

The time step should be small enough in order for the dynamics to be numerically stable. When the size n of the system, the noise strength η , the anharmonicity b or the Langevin friction γ are

increased, the time step should be reduced. Indeed, in all these cases, the energy of the system increases (at least locally). Due to nonlinearities, this energy may concentrate on a few sites, and hence trigger numerical instabilities. Such issues are not encountered with harmonic potentials, where some uniform stability condition is valid.

In the case $b = 1$ and $\epsilon = 0.1$, most of our computations have been done with $\tau = 0.05$. However, for the largest systems, and for the largest values of ϵ , we had to use the smaller value $\tau = 0.025$ (otherwise, the simulation blows up due to numerical instabilities, as for $n = 2^{14}$ and $\epsilon = 1$). For $b = 1$ and $\epsilon = 1$, that is a stronger noise at the boundaries thermostats, we also observe that we have to reduce the time step. We worked with $\tau = 0.025$ for all values of n . When b is increased from $b = 1$ to $b = 10$ (with $\epsilon = 0.1$), the potential energy becomes stiffer, and we again need to use a smaller time step. In the case $b = 10$ and $\epsilon = 0.1$, we worked with $\tau = 0.01$ for all values of n and ϵ , except for the large values of ϵ and when $n = 2^{13}$, for which we used $\tau = 0.005$.

Let us now describe two artifacts of the numerical results that occur when the time step is too large. Observing them in practice is an indication that the time step is too large and should be reduced. In Figure 2, we plot the Hamiltonian current as a function of the chain length n , for $b = 1$, $\epsilon = 1$ and $\epsilon = 1$, for two different time steps. These currents have been computed as the time averages (21) on simulations long enough. For $\tau = 0.05$, the current is not monotonically decreasing with n , which is clearly a numerical artifact. The simulation blows up for $n = 2^{14}$ and is stable for $n = 2^{13}$, but it is clear that the latter point cannot be trusted.

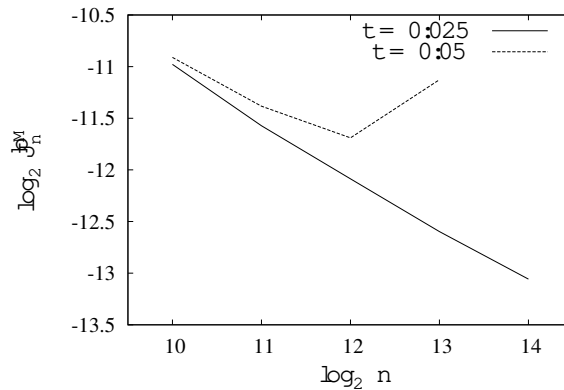


Figure 2: Hamiltonian current (21) as a function of the chain length n , for $\tau = 0.05$ and $\tau = 0.025$ (with $b = 1$, $\epsilon = 1$ and $\epsilon = 1$).

On Figure 3, we plot the temperature profile, at the end of the simulation ($T = M^{-1} \tau = 4.24 \cdot 10^7$), in the case of a chain of length $n = 2^{13}$ (with $b = 1$, $\epsilon = 1$ and $\epsilon = 1$). When we use $\tau = 0.025$, we obtain a decreasing temperature from the left end to the right end, which is in agreement with what is expected. When $\tau = 0.05$, the results are completely different, and physically unreasonable, which again shows that these results cannot be trusted.

3.2.2 Variability of the results

We mentioned earlier that we needed extremely long simulations to obtain a good accuracy. The reason for that can be well understood from Figure 4, on which we plot the instantaneous Hamiltonian current J_H^m (defined by (20)) and its time average (21) as a function of time, for a chain of length $n = 2^{14}$ (for the parameters $b = 1$, $\epsilon = 1$ and $\epsilon = 1$). We observe that J_H^m roughly oscillates between -0.02 and 0.02 , whereas its time average is close to 10^{-4} . Hence the variability of J_H^m is extremely large in comparison with its expectation. We hence need to run a very long simulation to be able to average out most of the fluctuation and obtain J_H^m with a good accuracy.

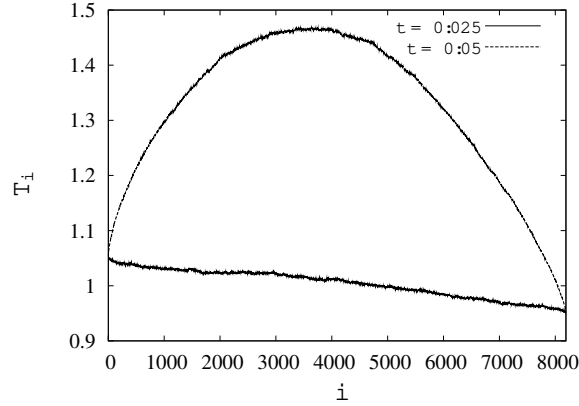


Figure 3: Averaged temperature profiles along the chain of length $n = 2^{13} = 8192$, for $t = 0.05$ and $t = 0.025$ (with $b = 1$, $\beta = 1$ and $\gamma = 1$) at the end of the simulation.

These heuristic considerations can be quantified by a simple computation. The standard deviation of the instantaneous current in Figure 4 is of the order of 0.02 , while the average value of the current is 10^{-4} . In addition, it is possible to estimate the typical correlation time τ_{corr} using block averaging (also called batch means in the statistics literature), see [11, 12]. Here, we obtain $\tau_{\text{corr}} \approx 10^3$. The time t_{req} required to obtain a 1% relative accuracy on the average current is such that

$$\frac{1}{\tau_{\text{req}}} = 0.01 : \tau_{\text{req}} = 100$$

This yields $t_{\text{req}} \approx 4 \times 10^{11}$. Since the time step is $\Delta t = 0.05$, this means that a huge number of time steps should be used to reach convergence.

For large values of n and large values of β , we observe that h^m is very small (see the numerical results below). Its accurate computation hence needs an even longer simulation time. In addition, the cost of the simulation of a chain, on a given time range, linearly increases with the size of the chain. This explains why computing the average currents for the longest chains is an extremely expensive task.

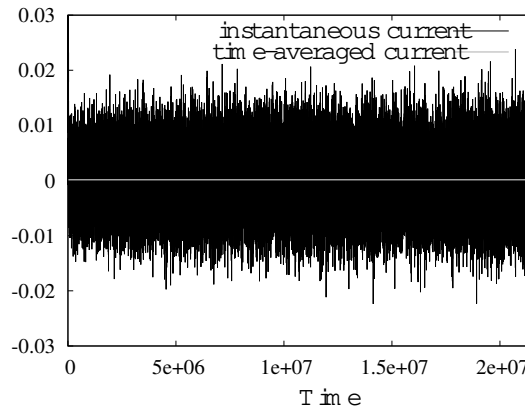


Figure 4: Instantaneous Hamiltonian current (20) and its time average (21) as a function of time, for a chain of length $n = 2^{14}$ (for the parameters $b = 1$, $\beta = 1$ and $\gamma = 1$).

	$(b = 1; \gamma = 1)$	$(b = 1; \gamma = 0.1)$	$(b = 10; \gamma = 0.1)$
0.001	0.10	{	{
0.01	0.11	0.17	0.25
0.1	0.32	0.30	0.32
1	0.44	0.44	0.43

Table 1: Conductivity exponent α , estimated from (22), for different values of γ and b , and different potential energies.

3.3 Numerical results

We represent the conductivity (22) as a function of the system length in Figure 5. We considered the choices $b = 1$ and $b = 10$ for $\gamma = 0.1$ to study the influence of the potential energy anharmonicity. We also simulated the system with $b = 1$ and $\gamma = 1$ to study how the results depend on γ . The total simulation time for each point ranges from $T = M \tau = 10^6$ to $T = 5 \cdot 10^7$, depending on the size n of the system.

The slope α , defined by (22), is estimated using a least square fit in a log-log diagram. This estimate is quite sensitive to the choice of the number of points entering the fitting procedure, and only the very first digits of the estimated slope are reliable. Theoretical results (see [2]) show that the exponent α is expected to be lower than 0.5. Our numerical results, gathered in Table 1, are in accordance with the theoretical upper bound.

We also observe that, for $\gamma = 1$, the value of α is close to 0.5. Now recall that, in the harmonic case $V(r) = ar^2$, the value of α is always equal to 0.5, independently of γ . This seems consistent with the fact that, for large values of γ , the precise details of the potential V do not matter (the dynamics is mostly governed by the stochastic terms), and the behaviour of the system is close to the harmonic behaviour.

4 Discussion of the numerical results

Several conclusions can be drawn from the numerical results given in the previous section:

- (i) The ballistic transport, observed in the deterministic Toda lattice, which is due to the complete integrability of the system [23], is broken by the presence of noise in the dynamics. Energy transport becomes superdiffusive, i.e. $\langle x^2 \rangle \sim n^\alpha$, with $\alpha \in (0; 0.5)$. For a low level of noise (small), this superdiffusive regime may be seen only for systems large enough ($n \geq 2^{12}$ or more, depending on the stiffness parameter b of the system and the coupling to the boundaries thermostat). The asymptotic regime in n for the conductivity is attained for smaller values of n when γ or b is larger, or when b is smaller.
- (ii) The value of α seems to depend on the noise strength γ in a monotonically increasing way. If $\langle G_n^K \rangle$ had the same behavior, this would suggest that increasing the noise induces a slower time decay of the current-current correlations, in contradiction with the naive intuition that a stronger noise enhances the decay of time correlations. We believe that noise tends to suppress scattering effects due to the nonlinearity of the interaction. Observe that, in the harmonic case $V(r) = ar^2$, the value of α is always equal to 0.5 and in particular does not depend on γ [1, 2, 16]. The dependence of the exponent α on the noise strength γ in the Toda case also contradicts general theories about the universality of α (see for instance [17]). These theories need then to be restricted to more specific dynamics.

acknowledgements This work is supported in part by the MEGAS non-thematic program (Agence Nationale de la Recherche, France).

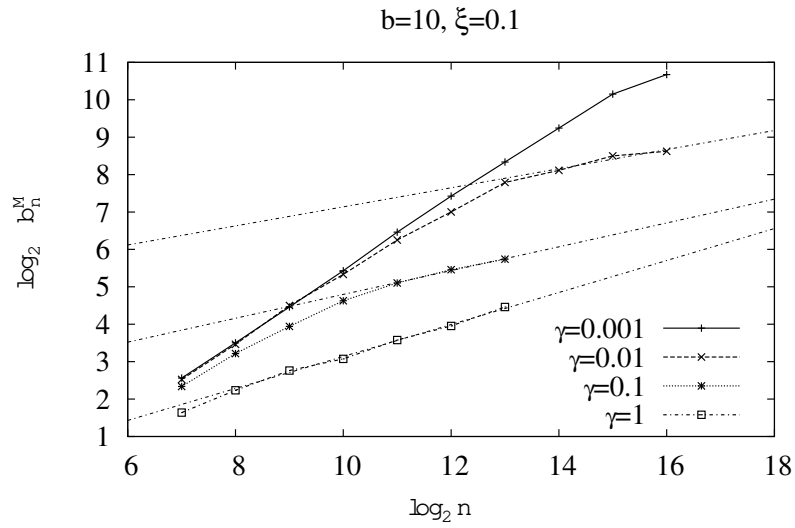
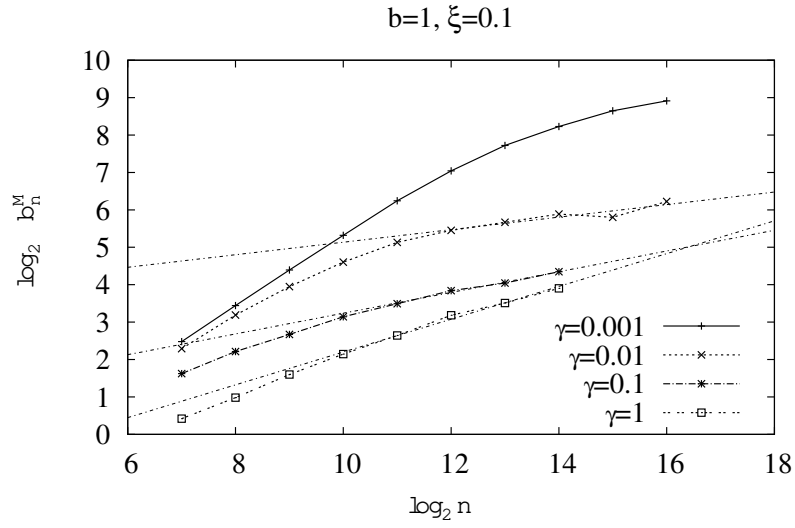
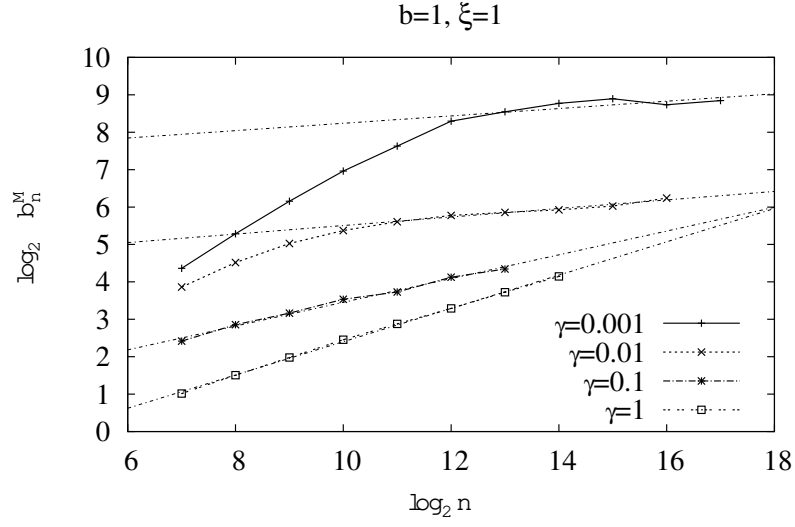


Figure 5: Conductivity b_n^M , defined by (22), as a function of the system size n .

References

- [1] G. Basile, C. Bernardin, and S. Olla. Momentum conserving model with anomalous thermal conductivity in low dimensional systems. *Phys. Rev. Lett.*, 96:204303, 2006.
- [2] G. Basile, C. Bernardin, and S. Olla. Thermal conductivity for a momentum conserving model. *Commun. Math. Phys.*, 287(1):67{98, 2009.
- [3] C. Bernardin and S. Olla. Fourier’s law for a microscopic model of heat conduction. *J. Stat. Phys.*, 121:271{289, 2005.
- [4] M. Bolsterli, M. Rich, and W. M. Visscher. Simulation of nonharmonic interactions in a crystal by self-consistent reservoirs. *Phys. Rev. A*, 1(4):1086{1088, 1970.
- [5] F. Bonetto, J. L. Lebowitz, and J. Lukkarinen. Fourier’s law for a harmonic crystal with self-consistent stochastic reservoirs. *J. Stat. Phys.*, 116:783{813, 2004.
- [6] F. Bonetto, J. L. Lebowitz, J. Lukkarinen, and S. Olla. Heat conduction and entropy production in anharmonic crystals with self-consistent stochastic reservoirs. *J. Stat. Phys.*, 134:1097{1119, 2009.
- [7] F. Bonetto, J. L. Lebowitz, and L. Rey-Bellet. Fourier’s law : a challenge for theorists. In A. Fokas, A. Grigoryan, T. Kibble, and B. Zegarlinsky, editors, *Mathematical Physics 2000*, pages 128{151. Imperial College Press, 2000.
- [8] A. Brunger, C. B. Brooks, and M. Karplus. Stochastic boundary conditions for molecular dynamics simulations of ST2 water. *Chem. Phys. Lett.*, 105(5):495{500, 1984.
- [9] P. Carmona. Existence and uniqueness of an invariant measure for a chain of oscillators in contact with two heat baths: Some examples. *Stoch. Proc. Appl.*, 117(8):1076{1092, 2007.
- [10] C. W. Chang, D. Okawa, H. Garcia, A. Majumdar, and A. Zettl. Breakdown of Fourier’s law in nanotube thermal conductors. *Phys. Rev. Lett.*, 101:075903, 2008.
- [11] H. Flyvbjerg and H. G. Petersen. Error estimates on averages of correlated data. *J. Chem. Phys.*, 91:461{466, 1989.
- [12] C. J. Geyer. Practical Markov chain Monte Carlo (with discussion). *Stat. Sci.*, 7(4):473{511, 1992.
- [13] T. Hatano. Heat conduction in the diatomic Toda lattice revisited. *Phys. Rev. E*, 59(1):R1{R4, 1999.
- [14] S. Lepri, R. Livi, and A. Politi. Heat conduction in chains of nonlinear oscillators. *Phys. Rev. Lett.*, 78(10):1896{1899, 1997.
- [15] S. Lepri, R. Livi, and A. Politi. Thermal conduction in classical low-dimensional lattices. *Phys. Rep.*, 377:1{80, 2003.
- [16] S. Lepri, C. Mejía-Monasterio, and A. Politi. A stochastic model of anomalous heat transport: analytical solution of the steady state. *J. Phys. A : Math. Theor.*, 42:025001, 2009.
- [17] O. Narayan and S. Ramaswamy. Anomalous heat conduction in one-dimensional momentum-conserving systems. *Phys. Rev. Lett.*, 89:200601, 2002.
- [18] L. Rey-Bellet. Open classical systems. *Lect. Notes Math.*, 1881:41{78, 2006.
- [19] Z. Rieder, J. L. Lebowitz, and E. Lieb. Properties of a harmonic crystal in a stationary nonequilibrium state. *J. Math. Phys.*, 8(5):1073{1078, 1967.
- [20] M. Toda. Solitons and heat conduction. *Physica Scripta*, 20:424{430, 1979.

- [21] L. Verlet. Computer "experiments" on classical fluids. I. Thermodynamical properties of Lennard-Jones molecules. *Phys. Rev.*, 159:98{103, 1967.
- [22] Z. L. Wang, D. W. Tang, X. H. Zheng, W. G. Zhang, and Y. T. Zhu. Length-dependent thermal conductivity of single-wall carbon nanotubes: prediction and measurements. *Nanotechnology*, 18:4757{14, 2007.
- [23] X. Zotos. Ballistic transport in classical and quantum integrable systems. *Journal of low temperature physics*, 126(3-4):1185{1194, 2002.